

IDENTIFICATION OF ACCESSORY PROTEINS AND THEIR IMPACT ON THE
EXPRESSION OF THE EPITHELIAL SODIUM CHANNEL (ENaC)

by

Oluwatoyosi Adewunmi, B.S

A thesis submitted to the Graduate Council of
Texas State University in partial fulfillment
of the requirements for the degree of
Master of Science
with a Major in Biochemistry
May 2017

Committee Members:

Rachell Booth, Chair

Ronald Walter

Karen Lewis

COPYRIGHT

by

Oluwatoyosi Adewunmi

2017

FAIR USE AND AUTHOR'S PERMISSION STATEMENT

Fair Use

This work is protected by the Copyright Laws of the United States (Public Law 94-553, section 107). Consistent with fair use as defined in the Copyright Laws, brief quotations from this material are allowed with proper acknowledgment. Use of this material for financial gain without the author's express written permission is not allowed.

Duplication Permission

As the copyright holder of this work I, Oluwatoyosi Adewunmi, refuse permission to copy in excess of the "Fair Use" exemption without my written permission.

AKNOWLEDGMENTS

First I would like to thank my primary advisor Dr. Rachell Booth. This was my first biomedical research experience and you were always patient and understanding. You have taught me so much about research and about myself and I could not have done this without you. I would like to thank the members of my committee as well, Dr. Karen Lewis and Dr. Ronald Walter for taking the time out of their busy schedule to advise me. I would also like to thank members of the Booth lab, in particular, Taylor Dismuke. You have become like a sister to me and made going to lab fun each day.

I would like to thank my family for giving me support from afar. Thank you for always keeping me in your prayers and pretending to be interested in my work even when you had no idea what I was talking about. Finally, I would like to thank the Texas Doctoral Bridge Program, and mentors Dr. Babatunde Oyajobi and Dr. Niquet Blake. I would not be here if it was not for you, so thank you for bringing me to Texas State and providing constant support and advice that has helped me immensely.

TABLE OF CONTENTS

	Page
AKNOWLEDGEMENTS	iv
LIST OF TABLES	vi
LIST OF FIGURES	vii
ABSTRACT	viii
CHAPTER	
1. INTRODUCTION	1
2. MATERIALS AND METHODS.....	14
3. RESULTS AND DISCUSSION.....	23
4. CONCLUSION.....	41
REFERENCES	42

LIST OF TABLES

Table	Page
1. CRISPR/Cas9 gRNA sequence	18
2. Deletion strains transformed with α -ENaC plasmid.....	24
3. Summary of deletion strain characteristics in yeast, mouse, and human.....	30
4. RT-PCR analysis of α -ENaC primer	38

LIST OF FIGURES

Figure	Page
1. Diagram of the nephron	2
2. Schematic illustration of the location and function of ENaC in epithelia	3
3. Genetic conservation in ENaC/DEG family	5
4. Proposed structure of human ENaC.....	6
5. Schematic presentation of regulation of the epithelial Na ⁺ channel (ENaC) through Nedd4–2 and (Sgk).....	9
6. CRISPR/Cas9 vector map.....	19
7. Serial dilution pronging assay of yeast deletion and wildtype strains expressing α -ENaC	25
8. Serial dilution pronging assay of yeast deletion strains conserved in mammalian systems and wildtype strains expressing α -ENaC	27
9. Growth curve of <i>S. cerevisiae</i> cells transformed with pYES2N/TA- alpha ENaC	28
10. Primary antibody screen against α -, β -, and γ -ENaC.....	33
11. Mpk _{ccd} cells transfected with EDEM3 CRISPR/Cas9 KO plasmid.....	34
12. Western blot of EDEM3 knockdown cell lysates	34
13. Western blot of CRISPR/CAS9 treated cells.....	35
14. Graph of band intensities of knockdown cells compared to control band.....	36
15. Standard curve of serial dilutions for α , β , γ and 18S primers.....	37
16. Alpha ENaC mRNA expression levels of treated Mpk _{ccd} cells	39

ABSTRACT

The epithelial sodium channel (ENaC) plays a crucial role in ensuring proper Na⁺ balance in the body. In the nephron, ENaC regulates the final 3-5% reabsorption of Na⁺ and is a limiting factor for Na⁺ reabsorption in the kidneys. Because of its role in the kidneys, ENaC is thought to be a critical component in the control of blood pressure. Though there have been several accessory proteins known to regulate ENaC function, there are still questions to be answered about the role other proteins play in ENaC trafficking and assembly. Understanding the mechanisms behind ENaC regulation will potentially provide insight into certain defects in the trafficking or assembly of the channel, and identify possible therapeutic targets. Through survival dilution growth assays in yeast deletion strains, several genes were shown to effect ENaC function in a high salt growth media. A yeast deletion strain expressing α -ENaC but lacking ER degradation enhancing alpha-mannosidase like protein 3 (EDEM3) showed an increase in the growth of yeast cells compared to wildtype. Similarly, a yeast deletion strain lacking nuclear protein localization 4 (NPL4) showed an increase in the growth of yeast cells compared to wildtype. The lack of growth inhibition may indicate a possible loss in ENaC function. A Syntaxin 3 yeast deletion strain expressing α ENaC resulted in decreased cell growth indicating a possible gain in ENaC function. Western blot and real time PCR analysis on the knockdowns of EDEM3, Syntaxin 3, and NPL4 using a CRISPR/Cas9 knockout plasmid in a Mpk_{ccd} mammalian cell line endogenously expressing $\alpha\beta\gamma$ ENaC, demonstrated a decrease of ENaC protein expression levels.

1. INTRODUCTION

The proper maintenance of water volume in the human body is integral for life. The balance of water is mainly dependent on the concentration of electrolytes moving in and out of cells. Sodium ions (Na^+) are the major ion of the extracellular fluid (ECF) and Na^+ reabsorption as well as total body Na^+ levels are the primary determinant of ECF volume.¹ The disruption of Na^+ levels, can lead to a wide array of diseases including hypertension. Hypertension affects over one billion individuals worldwide and is one of the major treatable risk factors in cardiovascular diseases, such as stroke, myocardial infarction, heart, and kidney failure diseases, all leading causes of death in the United States.^{2,3}

Na^+ enters epithelial cells through ion channels that typically span the membrane and are responsible for the regulation of ion movement in and out of the cell based upon an electrochemical gradient. Of these transmembrane proteins, the epithelial sodium channel (ENaC) plays a crucial role in ensuring proper Na^+ balance in the body. ENaC is a voltage-independent sodium channel that is located mainly in tight or high resistance epithelia and allows the passive transport of Na^+ into the epithelial cell from the lumen. ENaC is located in the apical membrane of many epithelial tissues throughout the body including the colon, sweat glands, salivary duct, and airway.⁴

Though ENaC has varying functions depending on where it is expressed in the body, ENaC's role in kidney reabsorption is significant. ENaC is present in the cortical collecting duct of the nephron of the kidney, where the final regulation of Na^+ excretion takes place.⁵ The three main processes of the kidney are filtration, reabsorption, and

secretion. In humans, the nephron (Fig 1), the functional unit of the kidney, is responsible for filtering approximately 180 L of fluid per day.²

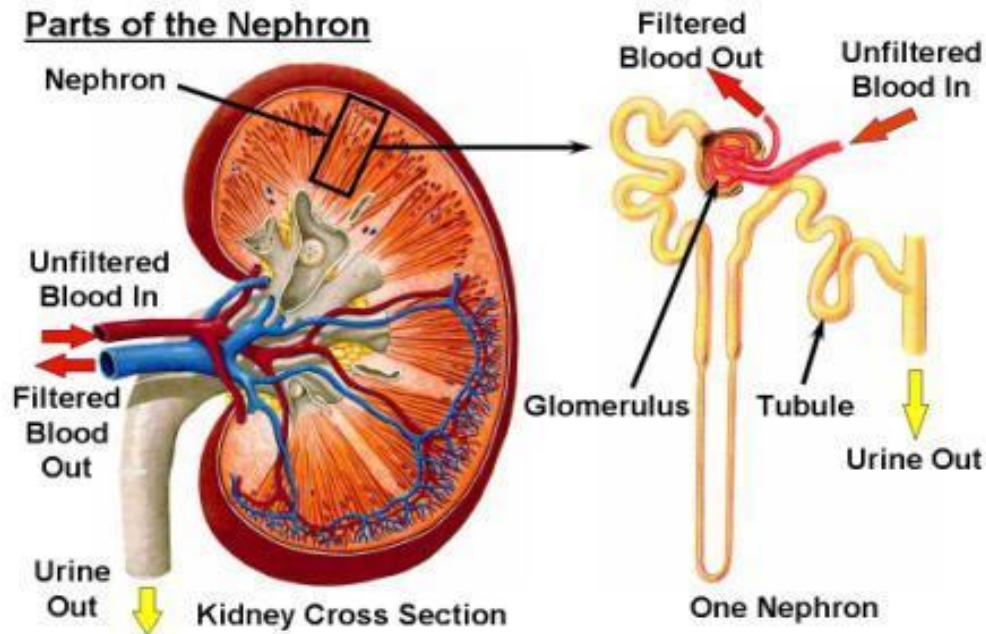


FIG 1. Diagram of the nephron. Unfiltered blood enters into the nephron from the circulatory system to be filtered and excreted. Before excretion, nutrients and ions required for homeostasis are reabsorbed back into the blood. Guyton, A.C. and Hall, J.E. (2006) *Textbook of Medical Physiology*. Philadelphia: Elsevier Saunders. pp.310.

Filtration via the kidney begins when blood enters the glomerulus. Approximately 20% of the blood gets filtered under pressure through the walls of the glomerular capillaries and is returned to circulation by the renal vein. The remaining filtrate passes to the proximal tubule (PCT) where reabsorption of key nutrients (including Na^+) takes place. From there the filtrate moves through the Loop of Henle that reabsorbs the filtrate while simultaneously removing water, resulting in concentration of ions. The concentrated filtrate then enters the cortical collecting duct of the distal tubules where the last 3-5% of sodium reabsorption occurs in what is considered to be the rate limiting step.^{1,2}

Since ENaC is a limiting factor for Na^+ reabsorption, it is thought to be a critical component in the indirect control of ECF volume, electrolyte balance, as well as blood pressure. The process of sodium ion absorption through the ENaC channel (Fig 2) begins when Na^+ enters the cell from the lumen through open channels. Once inside the epithelial cell, Na^+ is actively transported out of the cell and into the blood via the Na^+/K^+ ATPase. This ion movement also creates a driving force for potassium ions to be secreted into the lumen.^{6,7} The action of the Na^+/K^+ ATPase establishes a critical electrochemical gradient needed for Na^+ to enter the cell, and controls both the ion levels and the volume of fluid on either side of the basolateral membrane.^{8,1}

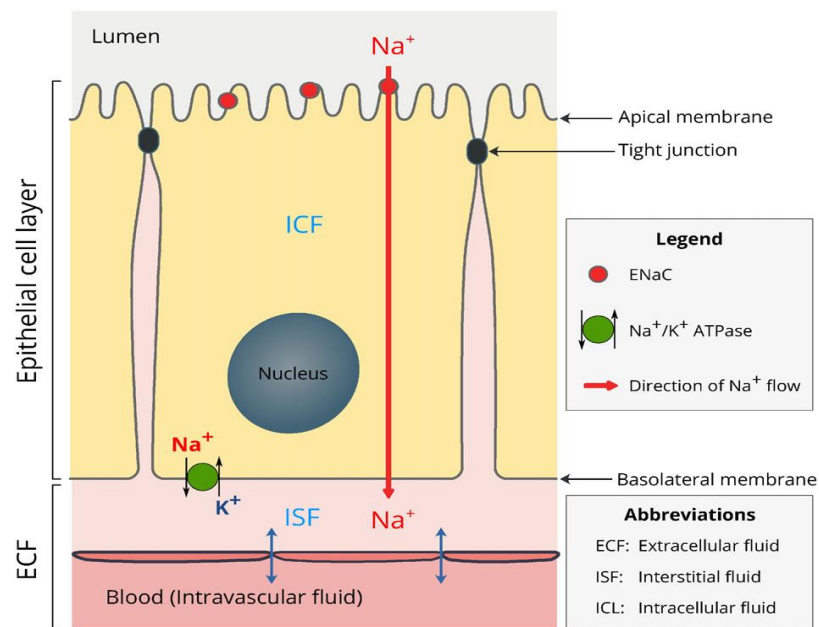


FIG 2. Schematic illustration of the location and function of ENaC in epithelia. Hanukoglu, I.; Hanukoglu, A., Epithelial sodium channel (ENaC) family: Phylogeny, structure-function, tissue distribution, and associated inherited diseases. *Gene* **2016**, 579 (2), 95-132.

ENaC is a member of the ENaC/degenerin superfamily of proteins, which is a structurally related family of non voltage-gated Na^+ channels found in various organisms.⁶ Others included in this superfamily are channels in *Caenorhabditis elegans*

(known as MECs and DEGs) that are involved in mechanosensation,^{9,10} a family of proteins in *Drosophila* that help aid airway fluid clearance, salt sensation, and detection of pheromones,⁶ and H⁺-gated acid-sensing ion channels (ASICs). ASICs are expressed in the mammalian central and peripheral nervous systems and play a role in pain sensation, mechanosensation, fear related behavior, and seizure termination.⁷ As shown in Fig 3, members of this superfamily all have four distinct, highly conserved domains: the cytoplasmic N-terminus and C-terminus, two short hydrophobic segments (TM1 and TM2) which are connected by a large extracellular loop. Members of the family are selective for sodium ions, though when compared to the other members, ENaC has a much greater selectivity. Through mutational studies of residues in the pore, the Gly/Ser-X-Ser tract in the TM2 of each subunit was found to be responsible for the channel Na⁺ selectivity and mutations at either the first or third positions in the tract lead to reduced Na⁺/K⁺ selectivity.⁶ Another characteristic shared by all ENaC/degenerin family members is their sensitivity to amiloride, with ENaC having the highest affinity.^{6,11} Amiloride is a diuretic that is used to manage hypertension and congestive heart failure. Amiloride competes with sodium and sterically blocks the pore of the channel.

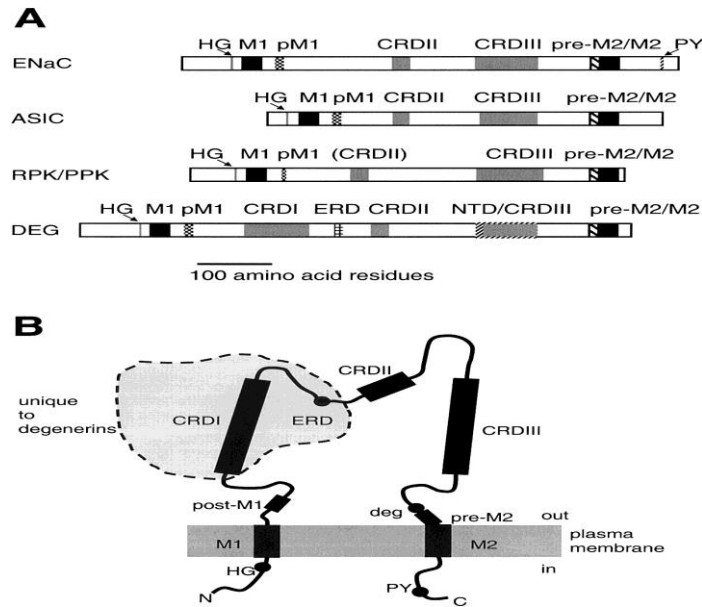


FIG 3. Genetic conservation in ENaC/DEG family. (A) Linear comparison of homologous regions within the primary sequence of different members of the superfamily. (B) Topology of an individual subunit. Kellenberger, S.; Schild, L., Epithelial sodium channel/degenerin family of ion channels: a variety of functions for a shared structure. *Physiol Rev* **2002**, 82 (3), 735-67

Though the structure of ENaC has yet to be elucidated, the recent crystallization of the chicken ASIC1, have given much insight to the structure of the channel. The crystal structure of chicken ASIC1 revealed the channel to be a homotrimer¹², and molecular modeling and site directed mutagenesis of conserved residues in ENaC have strengthened the idea that its structure is homologous to the ASIC1 channel.⁷ ENaC is assembled as a heterotrimer composed of three homologous subunits: α , β , and γ that are inserted into the membrane and arranged to form a central conductive pore¹³ (Fig 4). The α subunit alone has been shown to generate small amiloride-sensitive currents as well as subunit combinations of α - β or α - γ . However, maximal ENaC activity requires all three subunits to be present.⁸ In the human genome, the α subunit is encoded by SCNNA1A and is located on chromosome 6, whereas SCNN1B and SCNN1G, genes encoding β and γ subunits, respectively, are located on chromosome 16.⁷ The stoichiometric arrangement

of ENaC had previously been suggested to be $2\alpha:1\beta:1\gamma$ ⁸, however use of fluorescent labeled subunits and imaging of ENaC-antibody complexes by atomic force microscopy indicates that the subunits are assembled with a ratio of 1:1:1^{14,15}

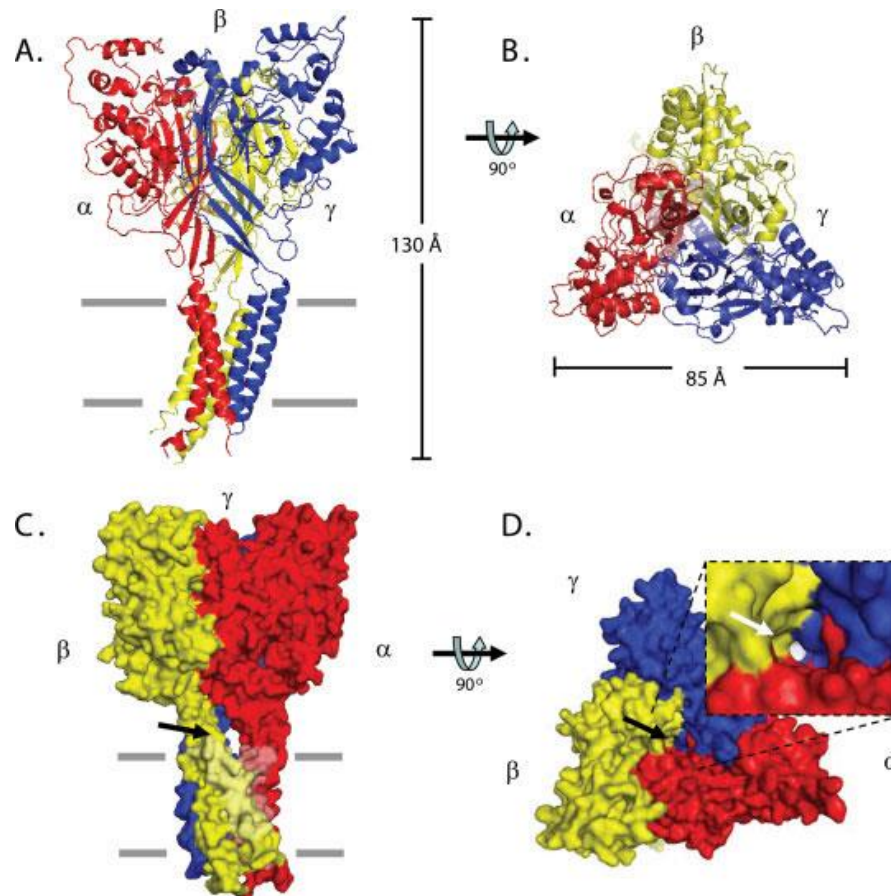


FIG 4. Proposed structure of human ENaC. A and B are ribbon diagrams of the proposed structure of ENaC showing the side view (A) and top view (B) of the channel. C and D are space filling models of ENaC from the side (C) and top view (D) Arrows show the predicted pore location in ENaC. Stewart, A. P.; Haerteis, S.; Diakov, A.; Korbmacher, C.; Edwardson, J. M., Atomic force microscopy reveals the architecture of the epithelial sodium channel (ENaC). *J Biol Chem* **2011**, 286 (37), 31944-52.

The expression of ENaC at the apical membrane of epithelia dictates the amount of Na^+ that is reabsorbed in the cortical collecting duct, with a greater number of channels leading to higher levels of reabsorption and vice versa. Thus Na^+ transport through ENaC

is regulated by the number of channels in the apical membrane, the single channel conductance, and probability of the channel being open.⁵ The number of channels present or the "open" channel probability can be adjusted through hormones, including aldosterone, insulin, vasopressin, and endothelin, either directly or through secondary messenger cascades.

Hormonal Regulation of ENaC

Aldosterone is a mineralocorticoid hormone known to regulate ENaC primarily through increasing transcription of the α ENaC subunit.¹⁶ Alternatively, ENaC trafficking is regulated by the renin-angiotensin-aldosterone cascade. The cascade is activated when there is a loss of blood volume or blood pressure causing the release of the enzyme renin from the kidneys. Renin then converts angiotensinogen into angiotensin I. Angiotensin I is converted to Angiotensin II through the angiotensin-converting enzyme (ACE) which stimulates the release of aldosterone. Aldosterone increases Na^+ transport by relocating ENaC subunits from the intracellular cytoplasmic pool to the apical membrane of the distal nephron, increasing channel density.⁵ Vasopressin increases expression of ENaC on the cell surface in response to changes in blood volume and osmotic pressure. When released by the hypothalamus, vasopressin binds to V2 receptors on the basolateral membrane of the cell activating adenylate cyclase which causes an increase in the level of intracellular cAMP.¹⁷ As a result, ENaC subunits stored in vesicle pools are mobilized by cAMP to the apical surface.^{18, 19} Insulin regulates ENaC expression through activation of phosphatidylinositol 3-kinase (PI3K). This activation increases colocalization of PI3K with ENaC, promoting translocation of ENaC to the apical membrane.²⁰ Endothelin is a negative regulator of ENaC that uses Src family kinases as intermediate signaling

proteins. Once activated by endothelin, Src family kinase activity decreases ENaC channel open time, inhibiting Na⁺ transport into the cell.²¹

Trafficking of ENaC

A point of possible regulation of ENaC is through trafficking, a very complex process that is still not completely understood. One widely studied accessory protein that is a part of ENaC trafficking is the neural precursor cell expressed developmentally downregulated gene 4-like (NEDD4-2). ENaC usually resides on the cell surface for a short period of time before it is internalized and degraded, and NEDD4-2 aids in the internalization process. It has been proposed that excess ENaC subunits synthesized in the endoplasmic reticulum but do not reach the plasma membrane are degraded through the ubiquitin proteasome pathway, while fully assembled ENaC proteins that are imbedded in the plasma membrane are monoubiquitinated by NEDD4-2 and targeted to endosomal/lysosomal degradation pathways.²² NEDD4-2 is comprised of four tryptophan based motifs called WW domains, and an ubiquitin ligase domain (HECT).¹ The WW domains of NEDD4-2 interact with proline rich regions, called PY motifs, found in the -COOH end of all three ENaC subunits.²³ The PY-motif -WW interaction brings the ubiquitin-protein ligase HECT domain into close proximity with the terminal ends of ENaC, leading to channel ubiquitination followed by endocytosis, and proteasomal degradation.¹

The NEDD4-2 and ENaC interaction can also be regulated physiologically through hormonal control. Serum and glucocorticoid-inducible kinase (SGK-1) is an accessory protein that can be activated in response to numerous stimuli including

aldosterone, insulin, and cAMP signaling pathways.²⁴ When stimulated, SGK-1 positively regulates ENaC activity, both directly and indirectly (Fig 4). In response to low blood pressure, aldosterone induces SGK-1, which decreases the affinity between NEDD4-2 and ENaC through phosphorylation. SGK-1 is shown to phosphorylate WW domains 2 and 3, producing a binding site for 14-3-3 family member proteins to bind to NEDD4-2 and sequester it away from ENaC.²⁴ Disrupting channel ubiquitination leads to greater ENaC density on the cell surface and an increase in Na⁺ intake.

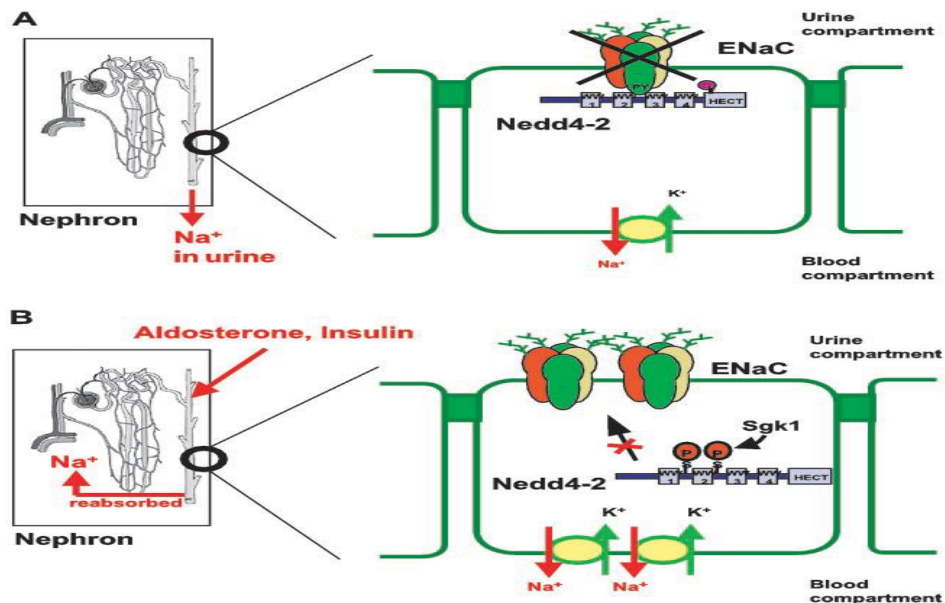


FIG 5. Schematic presentation of regulation of the epithelial Na⁺ channel (ENaC) through Nedd4-2 and (Sgk). A: ENaC cell surface expression is regulated through Nedd4-2 mediated ubiquitination. B: aldosterone induces expression of Sgk-1 and insulin also activates Sgk1 by phosphoinositol (PI)-3 kinase-dependent phosphorylation which leads to Sgk1-dependent phosphorylation of Nedd4-2. This reduces ENaC-Nedd4-2 interaction and causes reduced ENaC ubiquitination, increased ENaC density at the plasma membrane, and thus elevated Na⁺ reabsorption. Bruns, J. B.; Carattino, M. D.; Sheng, S.; Maarouf, A. B.; Weisz, O. A.; Pilewski, J. M.; Hughey, R. P.; Kleyman, T. R., Epithelial Na⁺ channels are fully activated by furin- and prostaticin-dependent release of an inhibitory peptide from the gamma-subunit. *J Biol Chem* **2007**, 282 (9), 6153-60

For more insight into regulation of ENaC, comparisons have been drawn between the assembly and trafficking of ENaC and similar proteins. *Rubenstein et.al* (2000) became interested in the seventy-kDa heat shock proteins because of their change in expression in response to sodium 4-phenylbutyrate (4PBA). 4PBA improves the intracellular trafficking of a common mutation of the cystic fibrosis transmembrane conductance regulator (CFTR) chloride channel,²⁵ and there is evidence it promotes ENaC trafficking as well.²⁶

The chaperone protein, Seventy-kDa heat shock cognate protein (Hsc70) has been shown to promote the internalization of active ENaC from the apical cell membrane as well as impair association of newly synthesized ENaC subunits, decreasing the amount of ENaC that reaches the cell surface.²⁷ Immunofluorescence microscopy and coimmunoprecipitation studies found that an increase in Hsc70 effected ENaC's association with certain Rab GTPases. Hsc70 increased the interaction of α and β subunits of ENaC with Rab7-containing late endosomes, targeting the protein for degradation. Hsc70 also decreased the interaction of α , β ENaC with Rab11, a component of recycling vesicles, impairing the proper recycling of ENaC.²⁷ Conversely, the homolog, 70-kDa heat shock protein 70 (Hsp70) increases ENaC activity by promoting interaction of newly synthesized ENaC with endoplasmic reticulum (ER) export machinery that facilitates delivery to the Golgi.²⁸ Increased Hsp70 was shown to increase ENaC association with COPII machinery, which is responsible for carrying cargo from the ER to the Golgi, therefore increasing the delivery of ENaC to the apical cell surface. Immunoprecipitation studies displayed an interaction between β -ENaC and

Sec24D, the cargo recognition component of COPII, which increased with Hsp70 overexpression.²⁸

Diseases Associated with ENaC

Significant changes in the structure of the ENaC protein can lead to functional failure and disease. The role of the ENaC channel in control of blood pressure can be seen through mutations in ENaC that lead to two rare genetic diseases: pseudohypoaldosteronism type 1 (PHA-1) and Liddle's Syndrome. PHA-1 is caused by a loss of function mutation leading to inactive ENaC channels that are unresponsive to aldosterone that occurs due to mutations of the α -, β -, or γ -ENaC subunit, or by mutations in the mineralocorticoid receptor.² This results in a loss of sodium and water volume in the blood vessels causing hypotension. PHA-1 is often known as a salt wasting disease, and is characterized by dehydration, hyponatremia, hyperkalemia and metabolic acidosis.³⁵ Conversely, Liddle's Syndrome, is a gain of function mutation that occurs in both the β and γ subunits. This mutation causes a continual reabsorption of Na^+ in the kidneys leading to a severe form of salt-sensitive hypertension. The gain of ENaC function is also correlated with hypokalemia, suppressed renin activity, and suppressed secretion of aldosterone.²⁹ Liddle syndrome is caused by missense mutations in the PY-motif of the β and γ subunits which leads to a loss of the motif in these subunits.⁷ The mutation of the PY-motifs disrupt their interaction with NEDD4-2 which causes an accumulation of active channels at the cell surface. Increased channel numbers lead to increased Na^+ reabsorption in the kidney, resulting in raised blood pressure and volume.⁷

Though there have been several accessory proteins known to regulate ENaC function questions remain about the role other proteins may play in ENaC trafficking and assembly. Further investigation of these proteins and how they interact with the ENaC channel may highlight multiple checkpoints in ENaC regulation. Understanding the mechanisms behind ENaC regulation will provide insight into the pathophysiological conditions caused from defects in the trafficking or assembly of the channel and identify targets for its therapeutic manipulation.⁵

Research Goals

Previous studies have identified accessory proteins that may possibly effect ENaC function³⁰. These studies were performed using a yeast deletion library, a library of yeast strains wherein each yeast cell has one non-essential gene knocked out.³¹. Numerous yeast deletion strains, as well as a wild type strain were transformed with a plasmid that can overexpress α -ENaC, causing yeast cells to become salt sensitive. Dilution growth assays have been carried out on these transformed deletion strains to assess how the deleted genes affect ENaC function in a high salt growth media. Genes chosen were known for their involvement in the trafficking and assembly of similar proteins and may be applicable to ENaC trafficking/assembly as well. Through survival growth assays, several deletion strains were identified that showed either decreased growth inhibition compared to the wild type strain indicating a loss of ENaC function, or increased growth inhibition compared to wild type indicating a gain of ENaC function. Yeast strain YOR036W (PEP12) was identified to have increased growth inhibition while strains YHR204W (MNL1) and YBR170C (NPL4) were identified to have a decreased growth inhibition.

With a difference in growth compared to wildtype observed in these yeast deletion strains, there was a possibility that the deleted genes influenced ENaC function. This warranted further evaluation in mammalian cell culture. Murine principal kidney cortical collecting duct (Mpk_{ccd}) cells were the immortalized mouse kidney cell line that endogenously expresses all three subunits of ENaC and can form a polarized monolayer³². A polarized monolayer allows for possible functional studies of ENaC using the change in voltage observed on either side of the layer. Silencing these genes of interest and further analysis of ENaC protein expression and function in Mpk_{ccd} cells will give insight into whether these proteins play a role in the assembly or trafficking of the ENaC channel. These studies will contribute to further understanding ENaC trafficking and transport to the cell surface of the epithelial membrane. Results will also shed further light on the complex roles accessory proteins may play in relationship to ENaC.

2. MATERIALS AND METHODS

Yeast Transformation

Alpha ENaC in pYES2NT-A was transformed into a deletion strain of wild type *S. cerevisiae* strain BY4742 using the following protocol. A pellet size of the yeast strain's frozen glycerol stock was incubated overnight in 4.0 ml of YPDA broth (1% w/v yeast extract, 2% w/v peptone, 0.02% adenine, and 2% w/v glucose) at 30°C with shaking. One milliliter of overnight culture was centrifuged at 14,000 x g for 30 seconds and the supernatant was discarded. Pellet formed was resuspended in 240 µl of 50% polyethylene glycol (PEG), 10 M of lithium acetate, 3.6 mg/ml of salmon sperm DNA (Agilent), 0.60% v/v of β-mercaptaethanol, ≥100 ng/µl of plasmid DNA and 69.5 µl of deionized water. The samples were then vortexed for 1 minute and incubated in a 42°C water bath for 20 minutes. After incubation, samples were centrifuged at 2000 x g for 2 minutes, supernatant removed, and the pellet was resuspended in 200 µl of deionized water. Approximately 150 µl of the sample was plated on to glucose minus uracil agar plates (2% w/v glucose, 0.67% w/v yeast nitrogen base, 0.01% w/v of leucine and tryptophan, 0.005% w/v histidine, 0.14 v% w/v yeast drop out media, and 2% w/v agar) and incubated for 2-4 days at 30°C. The ENaC in pYES2N/TA has a URA3 for selection in the minus uracil media used. Single colonies formed from transformation were chosen and streaked on to new plates.

Survival Dilution Pronging Assays

From the plates, a pea sized pellet of cells was dissolved in 500 μ l of deionized water to form a stock solution. From the stock solution, 25 μ l was diluted to 1/40 and sonicated for 8 seconds at 20% amplitude using a Sonics Vibracell Ultrasonic Processor (Newtown, CT). Cells were counted using a Reichert hemocytometer (Buffalo, NY) on an Olympus CKX41 light microscope (Melville, NY). Yeast cells from stock solutions were placed in a 96-well plate at a concentration of 1×10^7 cells per 220 μ l and serially diluted five-fold across the plate. Cells were then plated onto glucose minus uracil agar plates as a control and galactose minus uracil agar plates, which induces the expression of ENaC. Cells were also pronged on glucose and galactose plates with 0.75 M NaCl added to media. Plates were incubated at 30°C for 3 - 5 days and imaged using ChemiDoc XRS+ System Imager (Bio-Rad).

Growth Curve Assay

Individual deletion strains were incubated in 15 mL of glucose - uracil media for 24 hours at 30°C with shaking. The OD₆₀₀ was measured using a Bio-Rad Smart Spectrophotometer (Hercules, CA) and the amount needed to inoculate a 100 ml culture of galactose-uracil synthetic media so that the OD₆₀₀ was approximately equal to 0.2 was calculated. The amount of overnight culture was then centrifuged at 1500 x g for 5 min, supernatant discarded and resuspended in 100 mL of galactose-uracil media. OD₆₀₀ was taken initially at the 0 hr and cultures were then placed in a Precision Scientific 360 Orbital Shaker Water Bath at 30°C. OD₆₀₀ was measured every three hours until cells

reached the beginning of stationary phase, which was when the OD₆₀₀ of the last two time points did not have a difference greater than 0.3 AU.

Sequence Analysis

The protein sequence for each gene deleted in the yeast strains of interest was found using the *Saccharomyces* Genome Database (www.yeastgenome.org). The mouse and human homologs were then identified from the yeast protein sequence using the Basic Local Alignment Search Tool (BLASTp) for standard proteins provided by the National Center for Biotechnology Information (www.ncbi.nlm.nih.gov).

Cell Culture

Complete media

Mpk_{ccd} cells were generously donated by the Dr. James Stockand at the University of Texas Health Science Center San Antonio. Cells were cultured in the following media recipe: 1:1 ratio of Dulbecco's Modified Eagle's Medium (DMEM) (Corning Life Sciences, Tewksbury, MA) and Ham's F-12 (Corning Life Sciences), 50 nM dexamethasone (Sigma-Aldrich, St. Louis, MO), 1 nM triiodothyrodine (EMD Millipore, Darmstadt, Germany), 10 ng/ml Epidermal Growth Factor (EGF) (Sigma-Aldrich), 5 µg/ml Insulin/Transferin/Selinate (Sigma-Aldrich), 20 mM D-glucose (BD, Franklin Lakes, NJ), 2% v/v fetal bovine serum (FBS) (ThermoFisher Scientific, Rockford, IL), 2 mM glutamine (Corning Life Sciences), and 20 mM HEPES (Sigma-Aldrich).

Initiating Cell Culture

A vial with cells stored in media and 5% DMSO was quickly thawed at 37° C. The media/DMSO was then diluted in complete media pre-warmed to 37°C. Cells were then transferred into a T-25 cell culture flask (Corning Life Sciences) containing 10 mL of fresh media. Cells were incubated for 24 hours at 37°C with 5% CO₂, aspirated and then media was replaced. Media was subsequently changed every 2-3 days. Cells were passed when they reached 80 -100% confluency in the flask.

Passing Cells

Old media was aspirated and cells were rinsed with Dulbecco's Phosphate Buffer Saline (DPBS) without Mg²⁺ and Ca²⁺ (Corning Life Sciences). DPBS was removed and 3.0 ml of 1X Trypsin EDTA (Corning Life Sciences) was added to the cells and incubated at 37°C with 5% CO₂ for 5 minutes. Fresh media was added to the flask, pipetted up and down along the bottom to release any remaining cells on flask and to inactivate the trypsin. The cells were then centrifuged at 3,300 x g for 3 minutes. Media was aspirated, and the cell pellet was re-suspended in fresh media. Cells were then placed in T-75 stock flasks (Corning Life Science) for line maintenance or 6-well tissue plates or transwell plates (Corning Life Sciences) for experiments.

CRISPR/Cas9 Knockout Transfection Protocol

CRISPR/Cas 9 knockout plasmids were purchased through either GenScript or Santa Cruz Biotechnology. GenScript plasmids, encoding the Cas9 nuclease and a target-specific guide RNA(gRNA) were designed for maximum knockout efficiency (Table 1). Santa Cruz knock out plasmids utilize a pool of three gRNAs (Fig 6). In a tissue culture

plate (Corning) 1.5×10^5 - 2.5×10^5 cells were seeded in 3.0 ml of fresh media, and incubated for 24 hours in 37°C with 5% CO₂. In a sterile tube 3 µg of plasmid of DNA was mixed with 3 µl of Lipofectamine LTX Plus Reagent (ThermoFisher Scientific), brought to 150 µl with plasmid transfection medium (Santa Cruz Biotechnology), and immediately vortexed to mix well. The mixture was incubated for 5 minutes at room temperature. In a second tube, 6-15 µl of Lipofectamine LTX reagent (ThermoFisher Scientific) was diluted with 135-144 µl plasmid transfection medium (Santa Cruz Biotechnology) to reach a volume of 150 µl, vortexed immediately and left to stand for 5 minute in room temperature. Plasmid DNA complex (tube 1) was then added dropwise to Lipofectamine LTX reagent (tube 2) and incubated for 5 minutes at room temperature. Cells were aspirated, replaced with fresh media, and DNA-reagent complex was added dropwise to each well. Plate was incubated at 37°C with 5% CO₂ for 1-3 days. All three plasmids used were GFP labeled and cells were checked daily for fluorescence, indicating uptake of the plasmid. The volume of Lipofectamine LTX reagent that displayed ideal fluorescence was 7.5 µl and this volume was used for further transfections. Once fluorescence was observed cells were lysed for further analysis.

Table 1. CRISPR/Cas9 gRNA sequence

Gene Target	Guide RNA Sequence	Company
EDEM3-1	AGGAAGCCATGAAGACCGAA	Genscript
EDEM3-2	GACTGGGTGCGCAAAGACAG	Genscript

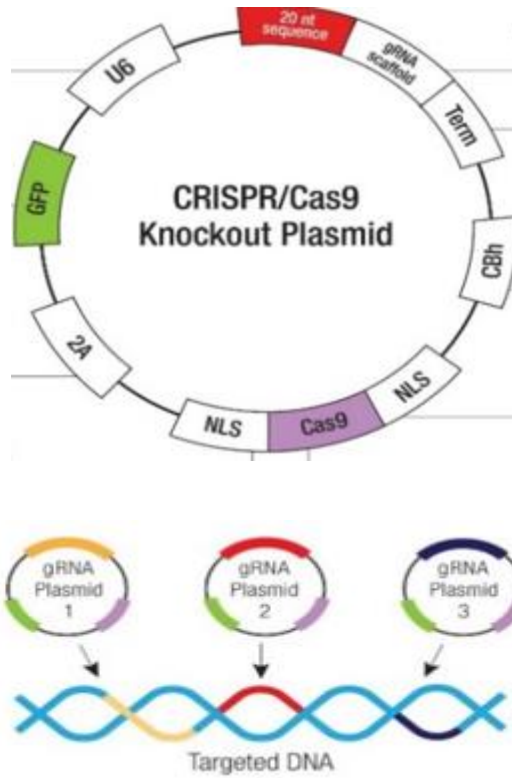


FIG 6. CRISPR/Cas9 vector map. Vector map of plasmids ordered from Santa Cruz Biotechnology. Syntaxin 3, NPL4, and a CRISPR negative control were plasmids ordered. <https://www.scbt.com/scbt/product/Npl4-crispr-knockout-and-activation-products>.

Cell Lysis

Mpk_{ccd} cells were rinsed with 10 mL of DPBS and treated with gentle lysis buffer (GLB) (76mM NaCl, 50 mM Tris-HCl, 2 mM ethylene glycol tetraaceticacid (EGTA), 1% NP-40 v/v, 10% v/v glycerol) and 1 mM phenylmethylsulfonylfluoride (PMSF) or RIPA buffer (10 mM Tris-Cl (pH 8.0), 1 mM EDTA. w/v, 1% Triton X-100 v/v, 0.1% sodium deoxycholate w/v 0.1% SDS w/v, 140 mM NaCl, 1 mM PMSF). Cells were scraped, incubated overnight at 4°C, and centrifuged at 3,300 x g for 5 minutes the next day. The supernatant was removed and stored at -4°C or used for experiments.

BCA Assay

A bicinchoninic acid assay (BCA) assay (ThermoFisher Scientific) was used to determine protein concentration of cell samples. In a 96-well plate 25 μ l of BSA standards at a concentration of 0, 0.025, 0.125, 0.25, 0.5, 0.75, 1.0, 1.5 and 2.0 μ g/ μ l was added. Protein samples with a 1:10 and 1:25 dilution was also placed into wells, and then the 200 μ l of BCA reagent was added to each well and incubated at 37°C for 30 minutes. Absorbance was measured at 562 nm using a Bio-Rad plate reader. A standard curve was created in Microsoft Excel using BSA standard concentrations as the x-axis and measured absorbance as the y-axis and used to calculate protein concentration of each sample.

Western Blotting and Development

Whole cell lysate (50-100 μ g), 1X NuPage LDS sample buffer (Invitrogen), 5% v/v beta-mercaptoethanol were mixed and incubated at 95°C for five minutes. Samples were loaded onto a sodium dodecyl sulfate polyacrylamide gel electrophoresis (SDS-PAGE) gel consisting of a 4% stacking gel (30 % v/v bis-acrylamide, 0.5 M Tris-HCl, pH 6.8, 10 % v/v SDS, 0.1 % v/v TEMED, and 10% w/v ammonium persulfate) and a 7.5% resolving gel (30 % v/v bis-acrylamide, 1.5 M Tris-HCl pH 8.8, 10 % v/v SDS, 0.05 % v/v TEMED, and 10% w/v ammonium persulfate). The gel was run at 120 volts for 60-75 minutes in 1X running buffer (25 mM Tris-base, 1.9 M glycine, and 0.1 % v/v SDS, pH 8). Gel was then transferred onto a nitrocellulose membrane using a Bio-Rad Trans-Blot Turbo Kit (Hercules, Ca) and the Bio-Rad Trans-Blot Turbo Transfer System (Hercules, Ca) set to 1.3 amps/ 25 volts for 30 minutes. After transfer, membrane was incubated in 5 mL of blocking solution (5% w/v non-fat dry milk in Tris-Buffered Saline

and 0.1% (v/v) Tween 20 (TBST)) for 30 minutes while being agitated. After blocking solution was discarded, α -ENaC antibody (ThermoFisher Scientific, catalog # PA1-9204) at a 1:5000 dilution was added to membrane and left to incubate at 4°C overnight while being agitated. After primary antibody incubation, membrane was washed three times in 20 ml TBST for 5 minutes before a goat anti-rabbit HRP conjugated secondary antibody (Jackson ImmunoResearch, West Grove, PA) was added. The membrane was incubated with secondary antibody for 1 hour and then rinsed three times with TBST for 5 minutes and once with 1X Tris-Buffered Saline (TBS) for 5 minutes. A 1:1 ratio of Western Lightning Plus-ECL Enhanced Chemiluminescence Substrate (PerkinElmer, Waltham, MA) reagents were added to the membrane, and membrane was left in the dark for 2 minutes. Reagents were removed and the membrane was then imaged using the ChemiDoc XRS+ System (Bio-Rad).

RT-PCR Expression Analysis

Total RNA from treated Mpk_{ccd} cells at 90-100% confluency was isolated using a AllPrep RNA/Protein isolation kit (Qiagen) and reverse transcribed to cDNA using a iScript cDNA synthesis kit (Applied Biosystems, Carlsbad, CA). The cDNA concentration was calculated using a Qubit machine. cDNA from each sample was analyzed using predesigned SYBR expression assays from Qiagen for mouse α -ENaC, mouse β -ENaC, mouse γ -ENaC, and a mouse 18S rRNA primer as a housekeeping gene. To determine the efficiency of the primers a serial dilution series (100 ng, 10 ng 1.0 ng and 0.1 ng), of untreated Mpk_{ccd} cDNA was run for the α , β , γ , primers and a 1:20 dilution for the 18S primer. The 18S primer is used as a reference gene since it is abundant in all cells. Real time PCR was then performed to analyze expression using

SYBR Green (Applied Biosystems) for detection on a 7500 fast RT-PCR machine (Applied Biosystems). Thermal cycling conditions consisted of a holding stage at 95°C for 20 s, and then 40 cycles of 95°C for 5 s and 60°C for 30 s. Each sample was analyzed in triplicate. After the PCR, a standard curve was created in Excel (Fig. 15) and the slope of the curve was used to find the efficiency of the primer using the equation $(10^{\frac{-1}{\text{slope}} - 1}) * 100$. With the primer efficiency established expression analysis was performed using 20 ng/μl of each sample.

3. RESULTS AND DISCUSSION

Accessory proteins play a large role in the assembly and trafficking of ENaC to the plasma membrane. However, understanding of which proteins interact with ENaC and to what extent they effect channel function is still fairly ambiguous. Investigation of proteins that effect the function or expression of the ENaC channel can offer multiple checkpoints in ENaC regulation. Through a preliminary yeast screening, several accessory proteins were found to impact ENaC function and investigated further in the Mpk_{ccd} kidney cell line. CRISPR/Cas9 was used to knockdown expression of these proteins and downstream qualitative as well as quantitative experiments were performed to assess how these knockdowns effected ENaC.

Yeast Dilution Pronging Assay

To determine accessory proteins that have an impact on ENaC function a preliminary yeast screening was performed using a yeast deletion library. Deletion strains chosen were chosen that play a role in the assembly, trafficking, or insertion of similar transmembrane proteins. Numerous yeast deletion strains (Table 2), as well as wild type BY4742 strain were transformed with a plasmid that overexpresses α -ENaC, causing yeast cells to become salt sensitive. Dilution growth assays were then carried out to assess how the deleted genes affected ENaC function in a high salt growth media. Cells that are expressing α - ENaC properly will show inhibited growth due to the protein's ability to draw in salt from the media, slowly inhibiting growth of the yeast cells. This growth inhibition is more pronounced when more salt is added to the media.

Table 2. Deletion strains transformed with α -ENaC plasmid

System Name	Description of Deleted Gene	Hit	Conserved in Mammalian Systems
YAL005C	Stress-Seventy subfamily A	no	
YLL024C	Stress-Seventy subfamily A	no	
YMR022W	Ubiquitin-Conjugating enzyme	no	
YMR264W	Coupling of Ubiquitin conjugation to ER degradation	yes	no
YOR036W	carboxyPEPtidase Y-deficient	yes	yes
YOL031C	Supressor of the Ire/Lhs1 double mutant	no	
YPL256C	Cyclin	no	
YPL240C	Heat Shock Protein	no	
YBR201W	Degradation in the Endoplasmic Reticulum	yes	no
YDR135C	Yeast Cadmium Factor	no	
YHR079C	Inositol Requiring	yes	no
YHR204W	Mannosidase-Like protein	yes	yes
YBL075C	Stress-Seventy subfamily A	no	no
YNL084C	Endocytosis defective	no	
YBR101C	Factor Exchange for Ssa1p	no	
YBR170C	Nuclear Protein Localization	yes	yes
YER103W	Stress-Seventy subfamily A	no	no
YBR097W	Vacuolar Protein Sorting	no	

The eighteen deletion strains tested (Fig 7) were screened for differences in salt sensitivity compared to wildtype yeast strain. Some strains exhibited growth inhibition in both glucose and galactose media, indicating that ENaC function was not the cause of the observed salt sensitivity, since ENaC expression was not turned on in glucose media.

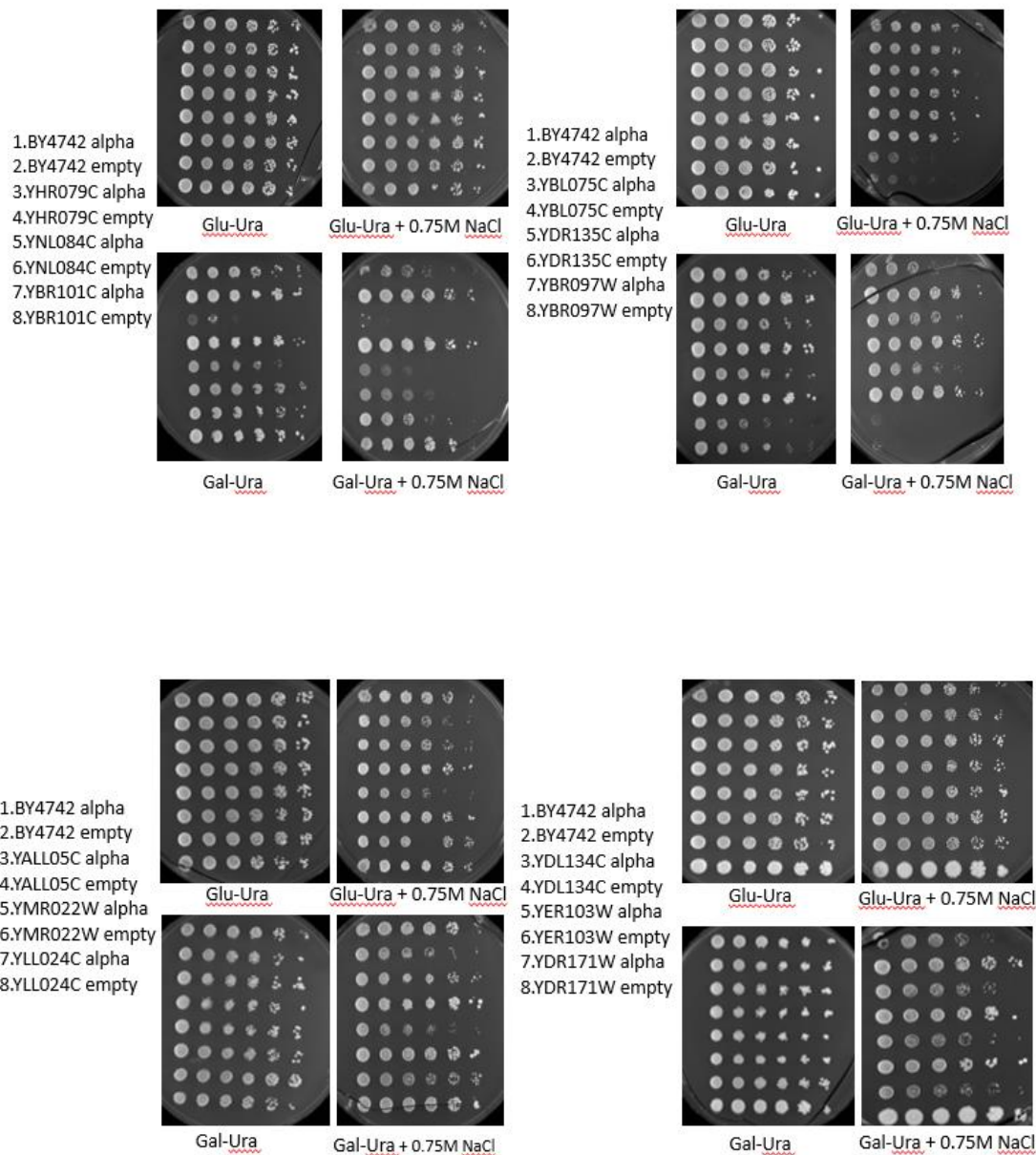


FIG 7. Serial dilution pronging assay of yeast deletion and wildtype strains expressing α -ENaC (continued on next page). Glu-Ura, Gal-Ura, Glu-Ura + 0.75M NaCl and Gal-Ura + 0.75 M NaCl plates. pYES2N/TA plasmids with α -ENaC and a pYES2N/TA empty vector plasmid were transformed into wildtype and deletion strains of yeast and grown for 3-5 days at 30.7 °C.

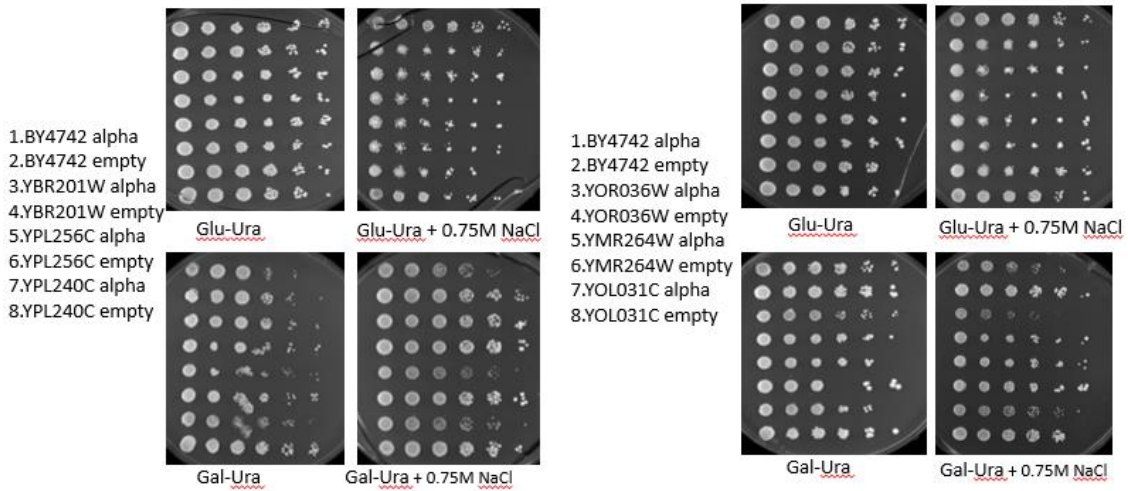
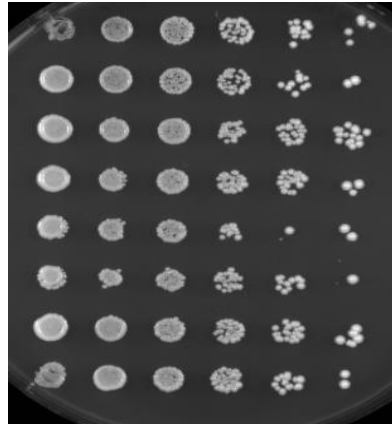


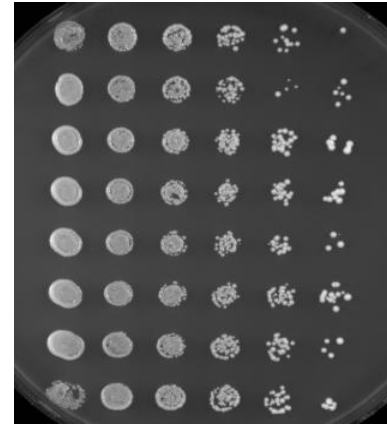
FIG 7 (continued). Serial dilution pronging assay of yeast deletion and wildtype strains expressing α -ENaC. Glu-Ura, Gal-Ura, Glu-Ura + 0.75M NaCl and Gal-Ura + 0.75 M NaCl plates. pYES2N/TA plasmids with α -ENaC and a pYES2N/TA empty vector plasmid were transformed into wildtype and deletion strains of yeast and grown for 3-5 days at 30.7 °C.

Several deletion strains displayed a change in growth inhibition compared to wildtype in galactose media, but not on glucose media, suggesting a possible change in ENaC function. However, only three of the genes in that subset of deletion strains are conserved in mammalian systems (Fig 8). The yeast deletion strain YOR036W (harboring a deletion in the yeast gene that codes for the protein PEP12) (Fig 6, row 5) was identified to have increased growth inhibition compared to wildtype yeast, indicating a possible gain of ENaC function. Conversely, YHR204W (deletion of the protein MNL1) and YBR170C (deletion of the protein NPL4) (Fig 6, rows 7 & 3) were identified to have increased growth compared to wildtype yeast, indicating a possible loss of ENaC function.

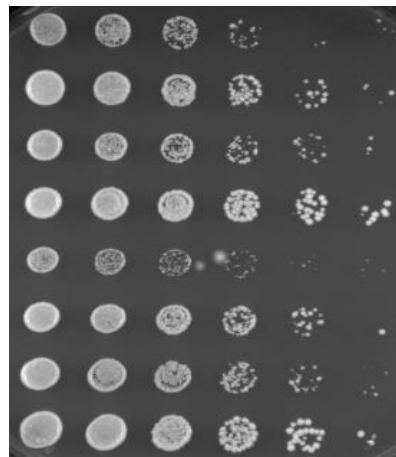
BY4742 alpha
 BY4742 empty
 YBR170C alpha
 YBR170C empty
 YOR036W alpha
 YOR036W empty
 YHR204W alpha
 YHR204W empty



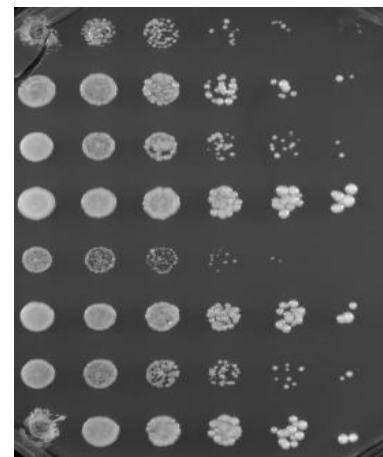
Glu-Ura



Glu-Ura + 0.75M NaCl



Gal-Ura



Gal-Ura + 0.75M NaCl

FIG 8. Serial dilution pronging assay of yeast deletion strains conserved in mammalian systems and wildtype strains expressing α -ENaC. Glu-Ura, Gal-Ura, Glu-Ura + 0.75M NaCl and Gal-Ura + 0.75 M NaCl plates. pYES2N/TA plasmids with α ENaC and a pYES2N/TA empty vector plasmid were transformed into wildtype and deletion strains of yeast and grown for 3-5 days at 30.7 °C.

Growth Curve Assays

To verify the qualitative results observed from the dilution growth assays, growth time courses were performed on each deletion strain expressing alpha ENaC. Cells were grown in selective media for up to 45 hours and growth curves (Fig 9) were created by measuring the absorbance at 600 nm every three hours.

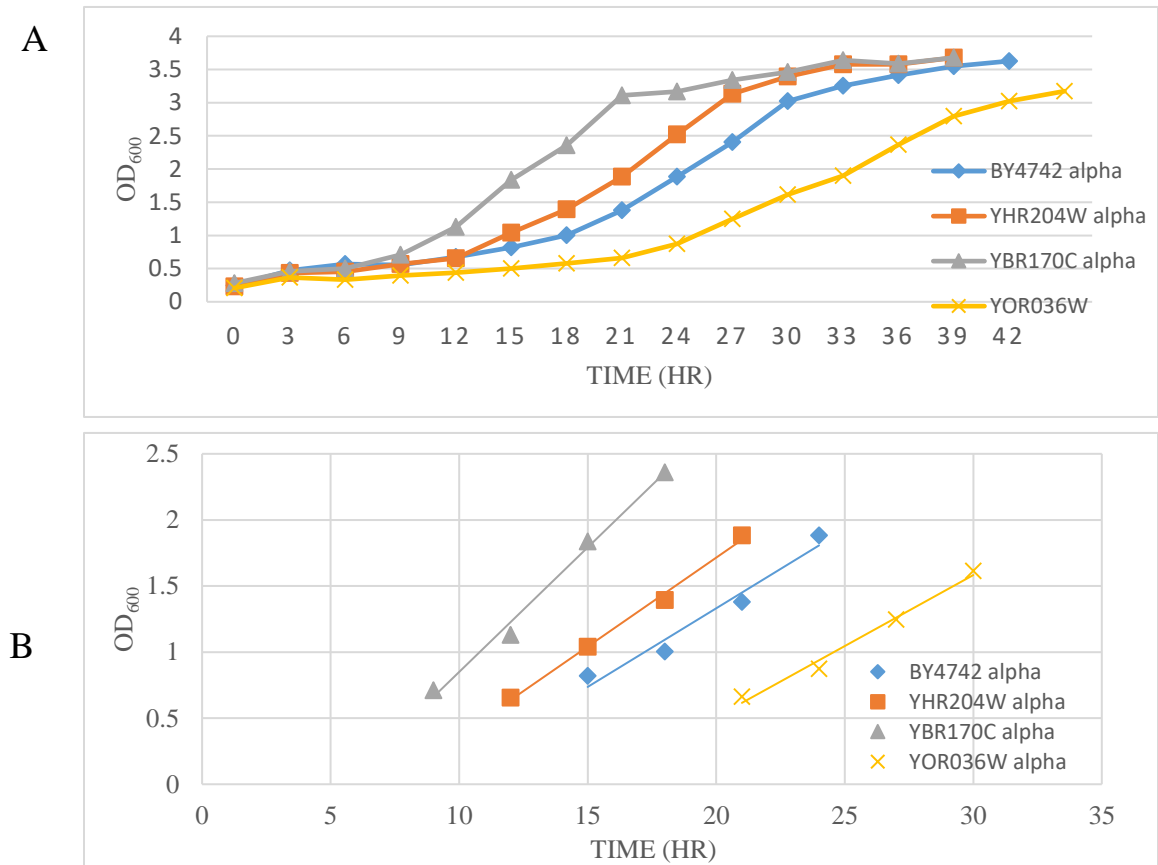


FIG 9. Growth curve of *S. cerevisiae* cells transformed with pYES2N/TA- alpha ENaC. The cells were grown at 30°C in galactose-uracil media for 40-45 hrs and the OD₆₀₀ was recorded at regular intervals. A. Growth curve of deletion alpha strains and wildtype alpha strain B. Linear fit of time points of each strain. Slope of YBR170C alpha is 0.19 AU/hr slope of YHR204W alpha is 0.13AU/hr, slope of BY4742 alpha is 0.12 AU/hr and the slope of YOR036W alpha is 0.11 AU/hr.

The slopes of the graph were calculated by fitting the curves to a linear trendline of time points during the yeast's log phase using Excel (Fig 9). YBR170C had the greatest rate of growth with a slope of 0.19 AU/hr which is consistent with the hypothesis that less salt is entering the cells causing a decrease in growth inhibition. However, YHR204W, YOR036W, and the wildtype BY4742 strain all had similar slopes at 0.13, 0.11, and 0.12 AU/hr respectively. Though the slopes in these deletions strains were similar to wildtype there was an observed difference in each strain's lag phase. YHR204W and YBR170C had shorter lag phases compared to BY4742 while YOR036W had a longer lag phase.

Sequence Analysis

The protein sequence of each deletion strain of interest was found using the *Saccharomyces* Genome Database and then each protein sequence was put into BLASTP against human as well as *Mus musculus* to identify the mammalian homolog (Table 3). The deleted gene in yeast strain YOR036W is the t-SNARE receptor protein PEP12 which has a 42% protein sequence identity and 68% homology with the human and mouse gene Syntaxin 3 (STX3). Syntaxin 3 is partly responsible for initiating as well as maintaining cell polarity necessary for protein trafficking, including vesicle fusion and exocytosis. Syntaxin 3 is a member of the syntaxin family and SNARE protein machinery which have been known to regulate the insertion and deletion of integral membrane proteins.³³ SNARE family member Syntaxin 1A has been shown to co-precipitate with the γ -subunit of ENaC and decreases the insertion of ENaC into the membrane.³⁴ Though Syntaxin 3 has been found to be localized to the apical membrane in cultured epithelial cells and principal cells of the rat cortical collecting duct³⁵, its

interaction and effect on ENaC function is still unknown. Syntaxin 3 has been shown to be necessary for regulated exocytosis of CFTR chloride channel in the small intestine, recruiting CFTR to the apical cell surface.³⁶ ENaC and the CFTR chloride channels have similar trafficking mechanisms including the use of the chaperone protein, Hsp70³⁷ so there is a possibility that Syntaxin 3 also plays a role in ENaC insertion in to the membrane as well.

Table 3. Summary of deletion strain characteristics in yeast, mouse, and human.

Strain	Mouse Protein (identity, homology)	Human Protein (identity, homology)	Description	Salt Sensitivity compared to wildtype
YOR036W	Syntaxin 3 (42, 68 %)	Syntaxin 3 (42, 68 %)	Member of SNARE family. Establishes and maintain polarity necessary for protein trafficking involving vesicle fusion and exocytosis.	Less
YHR204W	EDEM3 (36, 52%)	EDEM3 (35, 52 %)	ER degradation enhancing alpha-mannosidase like protein 3. Belongs to a family of proteins involved in ERAD of glycoproteins	More
YBR170C	NPLOC4 (39, 57 %)	NPLOC4 (34, 57%)	NPL4 homolog, ubiquitin recognition factor. Forms a stable heterodimer with Ufd1, and p97/VCP ATPase. Part of ERAD pathway.	More

The genes deleted in strains YHR204W and YBR170C are both a part of a process known as ER-associated degradation (ERAD). When proteins are not properly folded in the endoplasmic reticulum (ER), they are retrotranslocated to the cytosol and degraded by the proteasome. ERAD helps to ensure that only properly folded and assembled proteins are transported to their final destination through the secretory

pathway.³⁸ The deleted gene in YHR204W is an α mannosidase, which has a 35% protein sequence identity and 52% protein sequence homology with a human protein ER degradation enhancer, mannosidase α -like 3 (EDEM3). EDEM3 belongs to a family of proteins involved in the ERAD of glycoproteins. Mannose trimming by EDEMs of N-glycans on newly synthesized proteins plays a key role in the recognition and sorting of terminally misfolded glycoproteins for ERAD.⁴⁰ Misfolded proteins that have been trimmed are retrotranslocated into the cytosol, polyubiquitinated, and eventually degraded by the proteasome.³⁹

The deleted gene in strain YBR170C is nuclear protein localization 4 (NPL4) which has a 34% protein sequence identity and 57% protein sequence homology with the human gene NPL4 homolog, ubiquitin recognition factor (NPLOC4). NPL4 forms a stable heterodimer with Ufd1, which in turn binds to p97/VCP ATPase. p97 is a member of AAA ATPase family and, when complexed with Ufd1 and NPL4, is recruited to ubiquitinated substrates.⁴⁰ NPL4 acts as one of the adaptors that can link p97 to substrates, and the binding to ubiquitin step is mediated through a putative zinc finger in Npl4.⁴¹ The p97-Ufd1-Npl4 complex has been shown to be involved in the ERAD of inositol 1,4,5-trisphosphate (IP₃) receptors. IP₃ receptors form IP₃-gated channels in ER membranes and control the release of Ca²⁺. Coprecipitation studies revealed that p97-Ufd1-Npl4 interacted with IP₃ receptors inducing ubiquitination with the amount of co-precipitating p97-Ufd1-Npl4 complex correlating closely with the amount of ubiquitinated IP₃ receptor.⁴⁰ It has also been proposed that the p97-Ufd1-Nply complex is involved in the retranslocation of the ubiquitinated IP₃ from the ER to the cytosol for subsequent proteasomal degradation.⁴⁰

CRISPR/Cas9 Transfection and Western Blot Analysis

Initially, a *Xenopus laevis* kidney cell line (A6) was cultured, due to the ability of the cells to readily form a tight monolayer. However, the A6 cell line required *Xenopus* specific antibodies that were not available. Mouse kidney cell lines M-1, and Mpk_{ccd} were unable to form the tight monolayer required for functional studies, however protein expression could be analyzed using α -, β -, and γ - antibodies. Mpk_{ccd} cells were used for further transfection and analysis. To ensure that Mpk_{ccd} cells were endogenously expressing all three subunits of ENaC, an immunoblot for α -, β -, and γ - ENaC was performed. α -ENaC has a molecular weight of approximately 76 kDa, while both β - and γ -ENaC have slightly lower molecular weights of about 70 kDa. Western blot analysis was performed on 100 μ g of extracted protein from Mpk_{ccd} cells (Fig 9) using α - ENaC from Fisher Scientific (catalog # PA1-9204) and β -, γ - ENaC from Stressmarq (catalog #s SPC-404, and SPC-405). Lane 1 shows α -ENaC at higher weight above 70 kDa, while lane's 2 and 3 show β - and γ - ENaC at lower molecular weights of 55 and 70 kDa respectively. The higher α -ENaC molecular weight may be due to the glycosylated form of the protein being detected⁴² and the lower bands in this lane are thought to be cleaved ENaC products from the subunit. The cleaved product of the β -ENaC subunit was the only band detected and both the β - and γ - had a very faint signal compared to α -ENaC which is most likely due to less β - and γ - subunits in the Mpk_{ccd} sample.

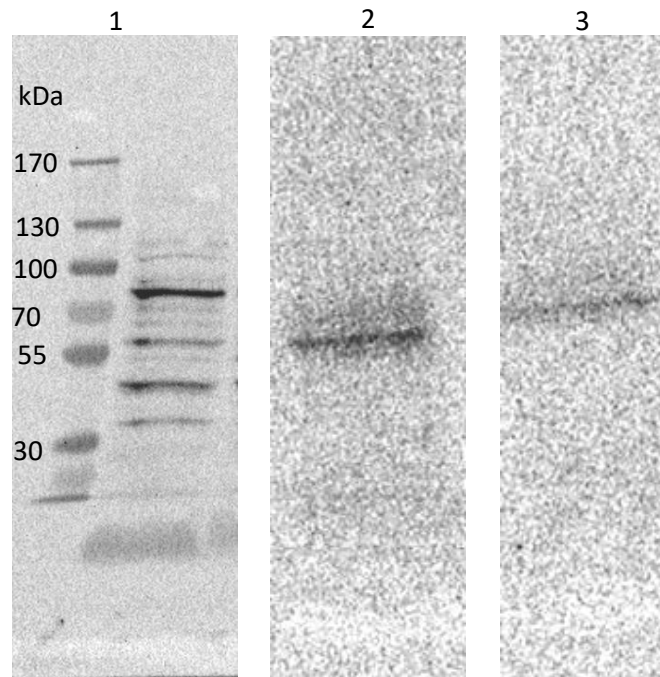


FIG 10. Primary antibody screen against α -, β -, and γ -ENaC. Three 100 μ g samples were run on same SDS PAGE gel, transferred to nitrocellulose membrane, and cut into three pieces. Lane 1 primary antibody α -ENaC (Fisher Scientific). Lane 2 primary antibody β -ENaC (Stressmarq). Lane 3 primary antibody γ -ENaC (Stressmarq).

Once detection of ENaC expression was confirmed in Mpk_{ccd} cells, cells were first transfected with two CRISPR/CAS 9 EDEM3 plasmids (E1 and E2) as well as a negative CRISPR control plasmid that encoded for a nonspecific gRNA. Plasmids used also expressed the fluorescent protein GFP, which allowed for visualization of cells that had taken up the plasmids (Fig 11). The two plasmids were transfected using 6-15 μ l of lipofectamine transfection reagent to determine the ideal ratio of reagent to media. When approximately 15-30% fluorescence was observed, cells were lysed with RIPA buffer, and 60 μ g of whole cell lysate was blotted against α -ENaC. The western blot shows that both EDEM3 knockdowns decreased ENaC expression compared to both untreated Mpk_{ccd} cells and negative CRISPR control (Fig 12).

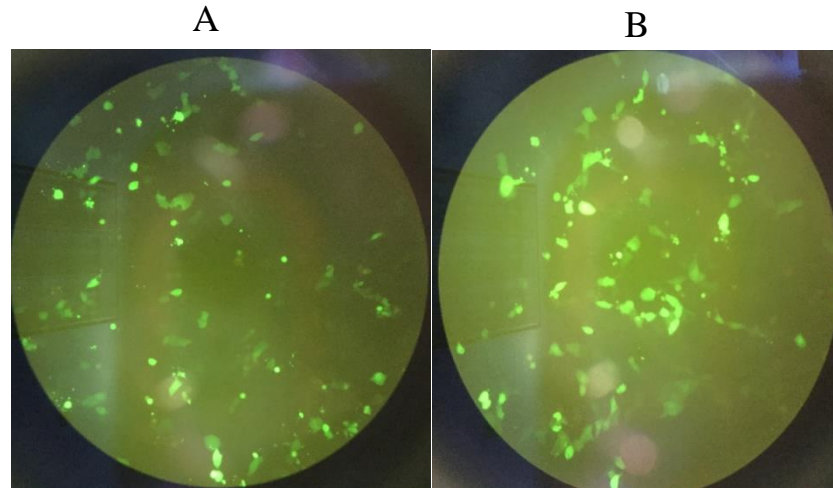


FIG 11. *Mpk_{ccd}* cells transfected with EDEM3 CRISPR/Cas9 KO plasmid. A. Cells transfected with EDEM3 vector 1 using 6 μ l of Lipofectamine LTX transfection reagent. B. Cells transfected with EDEM3 vector 2 using 9 μ l of Lipofectamine LTX transfection reagent.

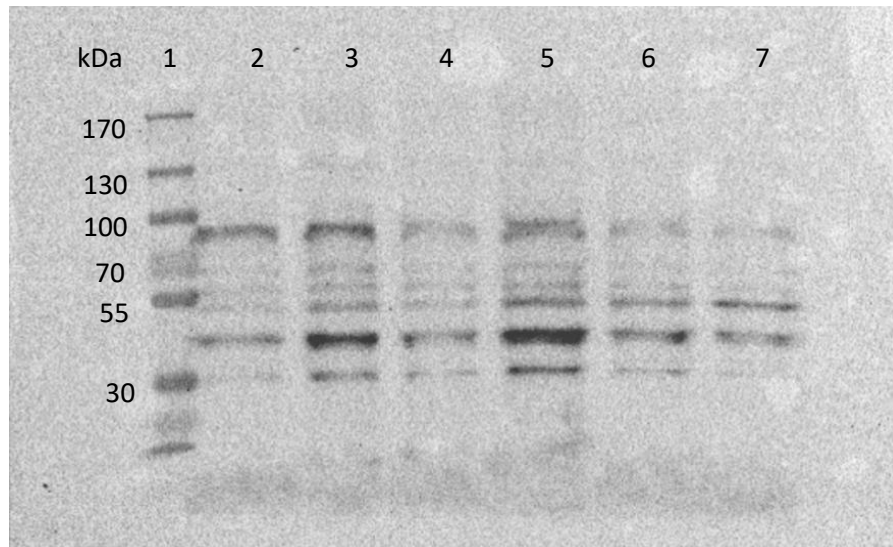


FIG 12. Western blot of EDEM3 knockdown cell lysates. Lane 1: ladder, Lane 2: *Mpk_{ccd}* cells untreated, Lane 3: CRISPR negative control, Lane 4: E1 with 6 μ l of transfection reagent used, Lane 5: E1 with 12 μ l of transfection reagent used, Lane 6: E2 with 9 μ l of transfection reagent used and Lane 7: E2 with 15 μ l of reagent used.

The western blot revealed that both EDEM3 gRNAs designed effectively decreased ENaC expression (Figure 12 lanes 4, 6, and 7). Lane 5 shows a discrepancy with other knockdowns and may possibly be due to a loading error where more than 60 μg were placed in the well. For further analysis, the bands in this blot were quantified relative to the CRISPR negative control using the ChemiDoc XRS+ System. Quantification showed that E2 transfected with 15 μl of reagent had the greatest decrease in ENaC expression, having only 28% intensity of the negative control band. Once the ideal transfection reagent concentration was determined all three plasmids were transfected into Mpk_{ccd} cells, lysed with RIPA buffer, and 50 μg of whole cell lysates were blotted against α -ENaC.

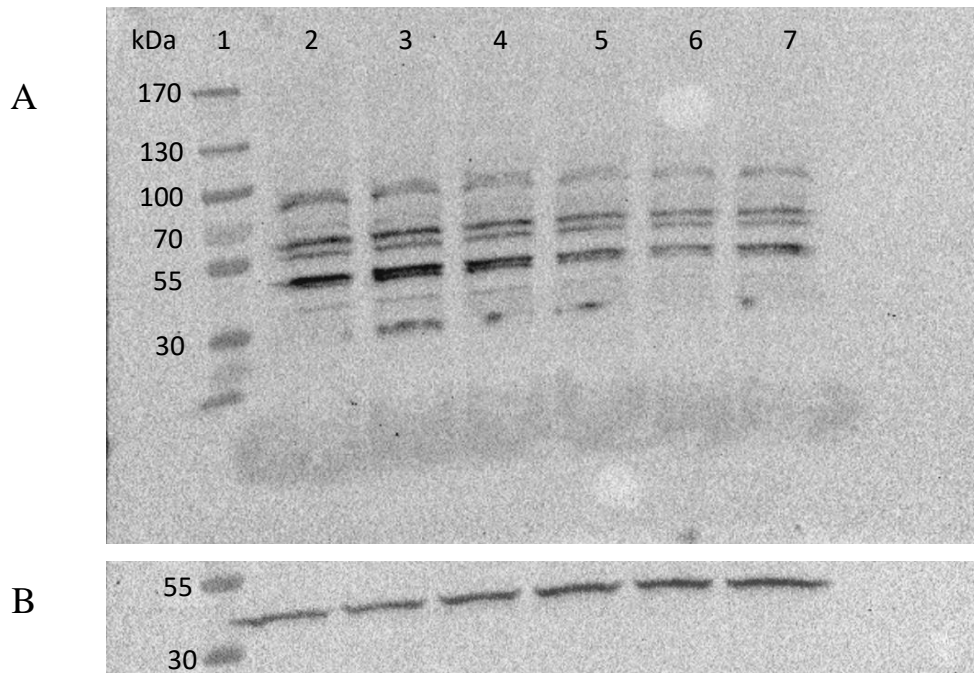


FIG 13. Western blot of CRISPR/CAS9 treated cells. A) Western blot shows that all three knockdowns decreased the expression of α -ENaC. Lane 1: Ladder, Lane 2: untreated Mpk_{ccd} cells, Lane 3: CRISPR negative control (reference), Lane 4: E1, Lane 5: E2, Lane 6: Syntaxin 3, and Lane 7: NPL4. B.) Western blot from panel A was stripped and reprobed for β -Actin to serve as a loading control.

The intensities of the bands were once again quantified (Fig 14) and this showed EDEM3 and NPL4 knockdowns decreased ENaC expression. Surprisingly Syntaxin 3 also showed a decrease in ENaC expression as well. In the yeast model Syntaxin 3 deletion caused an increase in ENaC function, which was hypothesized to be due to an increase in ENaC protein expression or function

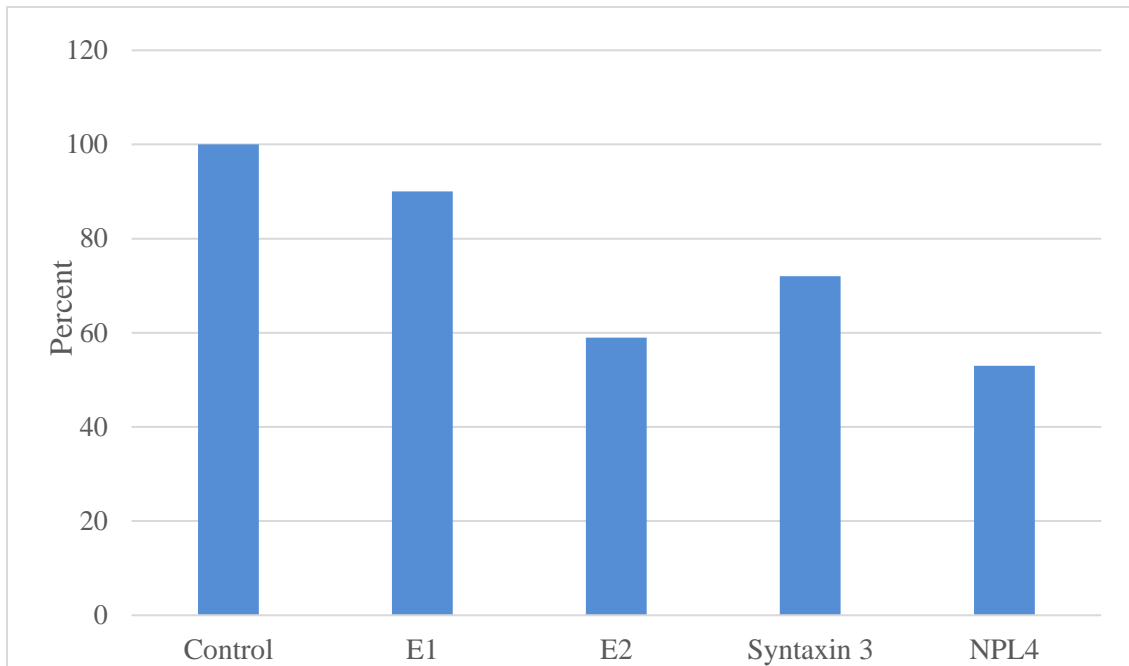


FIG 14. Graph of band intensities of knockdown cells compared to control band.

To further verify results shown in the western blot real time PCR was performed on transfected cells. RT-PCR is a sequence specific way to quantify mRNA levels in sample that also provides a high sensitivity.⁴³ Expression is measured through a parameter called the threshold cycle (C_T) value, which is the cycle in the PCR reaction where fluorescent signal is amplified above the background noise. The C_T value is the number of cycles of amplification it takes the sample to reach above the background. There is an inverse relationship between the C_T value and gene expression, where the

lower the value the greater amount of RNA is in the sample.⁴³ Relative PCR quantification is a way to measure and compare expression levels in target sample against a control sample and is what was utilized for this experiment. CRISPR/Cas9 treated cell expression levels were compared against the CRISPR negative control. The efficiency of primers used for a real time PCR reaction is critical to make sure that the data collected is accurate. In order to test the efficiency of the primers purchased, a serial dilution series of untreated Mpk_{cccd} cDNA was run with primers for with alpha, beta, gamma, and 18S. The 18S ribosomal RNA is used as an internal control because it is abundant in all cells. After the PCR a standard curve was created in Excel (Fig. 15) and the slope of the curve helps find the efficiency.

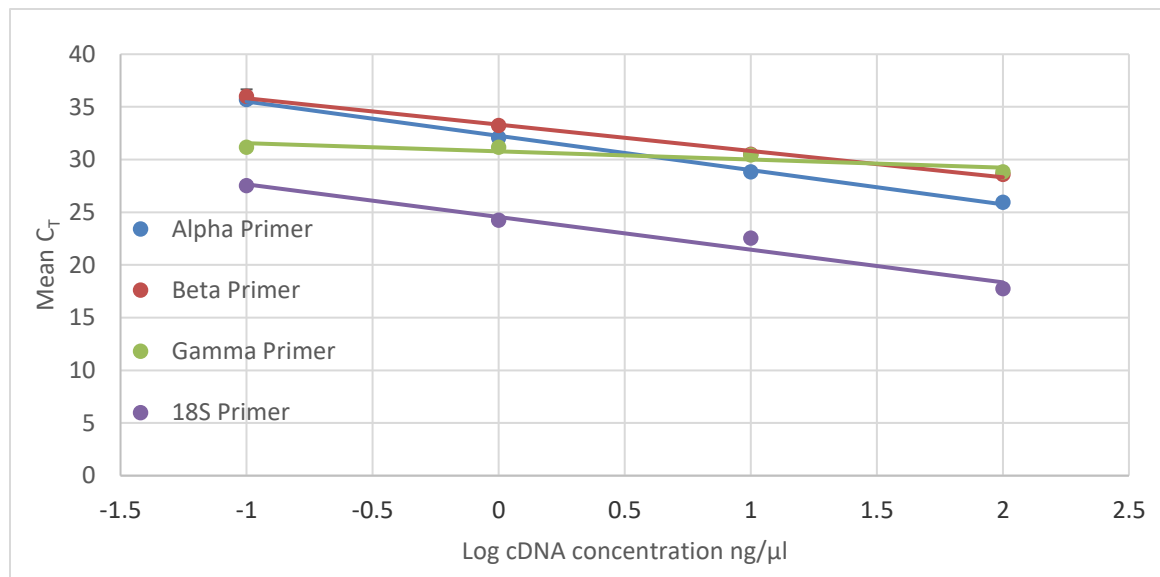


FIG 15. Standard curve of serial dilutions for α , β , γ and 18S primers. Efficiency of each primer was calculated. α -ENaC primer with a slope of -3.254 has an efficiency of 102%, β -ENaC primer with a slope of -2.499 has efficiency of 150%, γ - ENaC primer with a slope of -1.1651 has an efficiency is 621%, and 18S primer with a slope of -3.0998 has an efficiency of 110%

The equation $(10^{\frac{-1}{slope}} - 1) * 100$ was used to determine the efficiency. For RT-PCR primers must have an efficiency between 70-120% to be used for expression analysis. Both alpha and 18S primers had an acceptable efficiency at 102% and 110% respectively. The efficiency of the β -, and γ - primers were 150 % and 621% respectively and were not in the acceptable range. Once the efficiency of the primers was established an expression analysis of the treated cells was performed using the α -ENaC primer and 18S rRNA primer. An expression assay was performed using 20 ng/ μ l cDNA concentration of treated Mpk_{ccd} cells and analyzed (Table 4).

Table 4: RT-PCR analysis of α -ENaC primer

Name	ΔC_t	$\Delta\Delta C_t$	$2^{-\Delta\Delta C_t}$
Negative Control	5.39	0	1
Syntaxin 3	7.26	1.87	0.27
EDEM3	6.93	1.53	0.34
NPL4	7.61	1.22	0.21

First a change in C_T (ΔC_T) which is the difference between the C_T of sample and the C_T of 18S rRNA (housekeeping gene) was calculated. Then the difference between target sample and control sample was calculated giving the $\Delta\Delta C_T$. With the $\Delta\Delta C_T$, relative expression can be calculated using $2^{-\Delta\Delta C_t}$

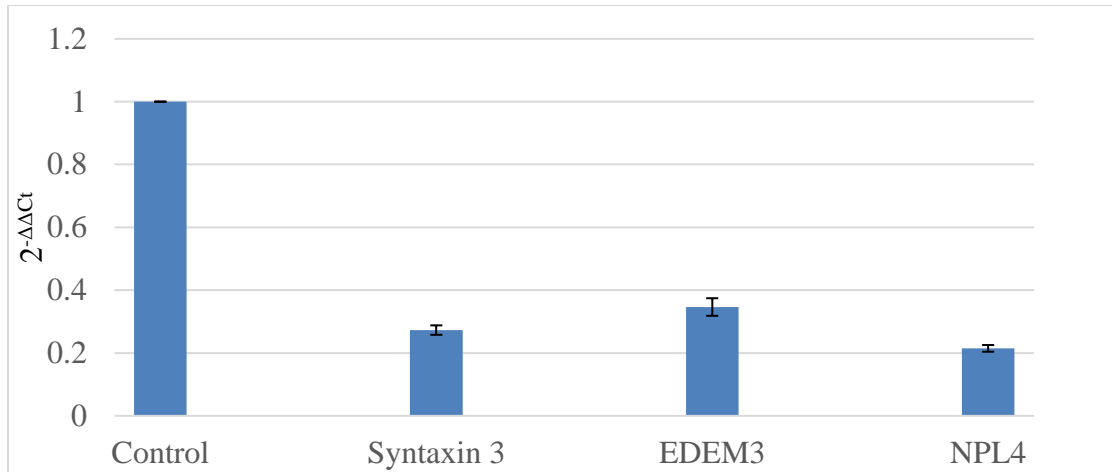


FIG 16. Alpha ENaC mRNA expression levels of treated Mpk_{cccl} cells.

The results in table 4 show a decrease in alpha ENaC mRNA levels in all three protein knockdowns verifying the decrease in protein expression observed through western blot analysis. Both EDEM3 and NPL4 have decreased mRNA expression compared to the control. In the yeast model, deletion of the homologs to these proteins caused a decrease in salt sensitivity indicating a possible loss of ENaC function. Results seen in mammalian cells are consistent with what was observed in yeast. Both EDEM3 and NPL4 are a part of the ERAD pathway play a role in the degradation of misfolded proteins. There is a possibility that the knockdown of these proteins causes ENaC to stay in the ER instead of being properly translocated to the cytosol for subsequent degradation. The accumulation of ENaC in the ER may disrupt the ERAD machinery and indirectly cause the decrease in ENaC expression. Syntaxin 3 also had less ENaC mRNA expression which differs from results observed in yeast. In the yeast model, deletion of the Syntaxin 3 homolog caused an increase in salt sensitivity indicating a possible gain in ENaC function. With the knockdown of Syntaxin 3 in mammalian cells showing a decrease in ENaC expression, it is a strong possibility that the protein's role in a

mammalian system differs from yeast. Syntaxin 3 has been shown to play a role in the insertion of other membrane proteins³⁶, and results of this study show that there is a possibility Syntaxin 3 also is a part of ENaC insertion in to the membrane. Results found in this study suggests further evaluation of these proteins and how they are affecting ENaC function will help expand the knowledge of how ENaC is trafficked to the membrane. A stable knockout line of each gene will be the most efficient way to continue because it will remove the variability that comes with multiple transfections. A knockout cell line will ensure that all cells have taken up the plasmid, and assays will reflect a 100% knockout population. Localization of ENaC in the knockout lines through confocal microscopy will build further understanding of the role these proteins play in ENaC trafficking. Electrophysiological studies will also provide insight into whether the knockouts are affecting the actual function of ENaC channels at the plasma membrane, or primarily affecting the expression of ENaC channels at the level of protein synthesis, folding, or trafficking.

4. CONCLUSION

The assembly and trafficking of the ENaC channel to the membrane is a complex process that still has many unknown variables. Knowledge of what proteins effect the function of ENaC, both directly and indirectly, will provide a better understanding of the channel and enhance our ability to manipulate its function. The survival growth assays of deletion yeast strains, was an inexpensive way to screen multiple proteins at a time, and with that screening three proteins that effected ENaC function was discovered.

Silencing of Syntaxin 3, EDEM3, and NPL4, through CRISPR/Cas9 knockdown, resulted in a decrease of α -ENaC expression compared to untreated cells or nonguided knockdown. Syntaxin 3 having a different result in mammalian cells than in yeast emphasizes the benefit of using multiple systems. Functional studies on a knockout cell line for each protein will show if they not only effect expression of ENaC but also the channels function. Confocal images of knockout cells will also provide insight on whether ENaC is making it to the membrane. Further study on how these proteins interact with ENaC will provide a better understanding of the trafficking machinery of the protein.

REFERENCES

1. Gormley, K.; Dong, Y.; Sagnella, G. A., Regulation of the epithelial sodium channel by accessory proteins. *Biochem J* **2003**, *371* (Pt 1), 1-14.
2. Rossier, B. C.; Staub, O.; Hummler, E., Genetic dissection of sodium and potassium transport along the aldosterone-sensitive distal nephron: importance in the control of blood pressure and hypertension. *FEBS Lett* **2013**, *587* (13), 1929-41.
3. Mozaffarian, D.; Benjamin, E. J.; Go, A. S.; Arnett, D. K.; Blaha, M. J.; Cushman, M.; de Ferranti, S.; Despres, J. P.; Fullerton, H. J.; Howard, V. J.; Huffman, M. D.; Judd, S. E.; Kissela, B. M.; Lackland, D. T.; Lichtman, J. H.; Lisabeth, L. D.; Liu, S.; Mackey, R. H.; Matchar, D. B.; McGuire, D. K.; Mohler, E. R., 3rd; Moy, C. S.; Muntner, P.; Mussolino, M. E.; Nasir, K.; Neumar, R. W.; Nichol, G.; Palaniappan, L.; Pandey, D. K.; Reeves, M. J.; Rodriguez, C. J.; Sorlie, P. D.; Stein, J.; Towfighi, A.; Turan, T. N.; Virani, S. S.; Willey, J. Z.; Woo, D.; Yeh, R. W.; Turner, M. B.; American Heart Association Statistics, C.; Stroke Statistics, S., Heart disease and stroke statistics--2015 update: a report from the American Heart Association. *Circulation* **2015**, *131* (4), e29-322.
4. Garty, H.; Palmer, L. G., Epithelial sodium channels: function, structure, and regulation. *Physiol Rev* **1997**, *77* (2), 359-96.
5. Butterworth, M. B., Regulation of the epithelial sodium channel (ENaC) by membrane trafficking. *Biochim Biophys Acta* **2010**, *1802* (12), 1166-77.
6. Kashlan, O. B.; Kleyman, T. R., ENaC structure and function in the wake of a resolved structure of a family member. *Am J Physiol Renal Physiol* **2011**, *301* (4), F684-96.
7. Hanukoglu, I.; Hanukoglu, A., Epithelial sodium channel (ENaC) family: Phylogeny, structure-function, tissue distribution, and associated inherited diseases. *Gene* **2016**, *579* (2), 95-132.
8. Kellenberger, S.; Schild, L., Epithelial sodium channel/degenerin family of ion channels: a variety of functions for a shared structure. *Physiol Rev* **2002**, *82* (3), 735-67.
9. Driscoll, M.; Chalfie, M., The mec-4 gene is a member of a family of *Caenorhabditis elegans* genes that can mutate to induce neuronal degeneration. *Nature* **1991**, *349* (6310), 588-93.
10. Huang, M.; Chalfie, M., Gene interactions affecting mechanosensory transduction in *Caenorhabditis elegans*. *Nature* **1994**, *367* (6462), 467-70.
11. Kellenberger, S.; Gautschi, I.; Schild, L., Mutations in the epithelial Na⁺ channel ENaC outer pore disrupt amiloride block by increasing its dissociation rate. *Mol Pharmacol* **2003**, *64* (4), 848-56.
12. Jasti, J.; Furukawa, H.; Gonzales, E. B.; Gouaux, E., Structure of acid-sensing ion channel 1 at 1.9 Å resolution and low pH. *Nature* **2007**, *449* (7160), 316-23.

13. Boiko, N.; Kucher, V.; Stockand, J. D., Pseudohypoaldosteronism type 1 and Liddle's syndrome mutations that affect the single-channel properties of the epithelial Na⁺ channel. *Physiol Rep* **2015**, *3* (11).
14. Staruschenko, A.; Adams, E.; Booth, R. E.; Stockand, J. D., Epithelial Na⁺ channel subunit stoichiometry. *Biophys J* **2005**, *88* (6), 3966-75.
15. Stewart, A. P.; Haerteis, S.; Diakov, A.; Korbmacher, C.; Edwardson, J. M., Atomic force microscopy reveals the architecture of the epithelial sodium channel (ENaC). *J Biol Chem* **2011**, *286* (37), 31944-52.
16. Verrey, F., Early aldosterone action: toward filling the gap between transcription and transport. *Am J Physiol* **1999**, *277* (3 Pt 2), F319-27.
17. Rossier, B. C., Epithelial sodium channel (ENaC) and the control of blood pressure. *Curr Opin Pharmacol* **2014**, *15*, 33-46.
18. Snyder, P. M., The epithelial Na⁺ channel: cell surface insertion and retrieval in Na⁺ homeostasis and hypertension. *Endocr Rev* **2002**, *23* (2), 258-75.
19. Edinger, R. S.; Bertrand, C. A.; Rondandino, C.; Apodaca, G. A.; Johnson, J. P.; Butterworth, M. B., The epithelial sodium channel (ENaC) establishes a trafficking vesicle pool responsible for its regulation. *PLoS One* **2012**, *7* (9), e46593.
20. Blazer-Yost, B. L.; Esterman, M. A.; Vlahos, C. J., Insulin-stimulated trafficking of ENaC in renal cells requires PI 3-kinase activity. *Am J Physiol Cell Physiol* **2003**, *284* (6), C1645-53.
21. Gilmore, E. S.; Stutts, M. J.; Milgram, S. L., SRC family kinases mediate epithelial Na⁺ channel inhibition by endothelin. *J Biol Chem* **2001**, *276* (45), 42610-7.
22. Staub, O.; Gautschi, I.; Ishikawa, T.; Breitschopf, K.; Ciechanover, A.; Schild, L.; Rotin, D., Regulation of stability and function of the epithelial Na⁺ channel (ENaC) by ubiquitination. *EMBO J* **1997**, *16* (21), 6325-36.
23. Kamynina, E.; Staub, O., Concerted action of ENaC, Nedd4-2, and Sgk1 in transepithelial Na⁽⁺⁾ transport. *Am J Physiol Renal Physiol* **2002**, *283* (3), F377-87.
24. Wiemuth, D.; Lott, J. S.; Ly, K.; Ke, Y.; Teesdale-Spittle, P.; Snyder, P. M.; McDonald, F. J., Interaction of serum- and glucocorticoid regulated kinase 1 (SGK1) with the WW-domains of Nedd4-2 is required for epithelial sodium channel regulation. *PLoS One* **2010**, *5* (8), e12163.
25. Rubenstein, R. C.; Zeitlin, P. L., Sodium 4-phenylbutyrate downregulates Hsc70: implications for intracellular trafficking of DeltaF508-CFTR. *Am J Physiol Cell Physiol* **2000**, *278* (2), C259-67.

26. Pruliere-Escabasse, V.; Planes, C.; Escudier, E.; Fanen, P.; Coste, A.; Clerici, C., Modulation of epithelial sodium channel trafficking and function by sodium 4-phenylbutyrate in human nasal epithelial cells. *J Biol Chem* **2007**, *282* (47), 34048-57.
27. Chanoux, R. A.; Shubin, C. B.; Robay, A.; Suaud, L.; Rubenstein, R. C., Hsc70 negatively regulates epithelial sodium channel trafficking at multiple sites in epithelial cells. *Am J Physiol Cell Physiol* **2013**, *305* (7), C776-87.
28. Chanoux, R. A.; Robay, A.; Shubin, C. B.; Kebler, C.; Suaud, L.; Rubenstein, R. C., Hsp70 promotes epithelial sodium channel functional expression by increasing its association with coat complex II and its exit from endoplasmic reticulum. *J Biol Chem* **2012**, *287* (23), 19255-65.
29. Busst, C. J., Blood pressure regulation via the epithelial sodium channel: from gene to kidney and beyond. *Clin Exp Pharmacol Physiol* **2013**, *40* (8), 495-503.
30. Lee, E. THE EFFECTS OF ACCESSORY PROTEINS ON ENaC FUNCTION. Texas State University, Texas, 2014.
31. Giaever, G.; Chu, A. M.; Ni, L.; Connelly, C.; Riles, L.; Veronneau, S.; Dow, S.; Lucau-Danila, A.; Anderson, K.; Andre, B.; Arkin, A. P.; Astromoff, A.; El-Bakkoury, M.; Bangham, R.; Benito, R.; Brachat, S.; Campanaro, S.; Curtiss, M.; Davis, K.; Deutschbauer, A.; Entian, K. D.; Flaherty, P.; Foury, F.; Garfinkel, D. J.; Gerstein, M.; Gotte, D.; Guldener, U.; Hegemann, J. H.; Hempel, S.; Herman, Z.; Jaramillo, D. F.; Kelly, D. E.; Kelly, S. L.; Kotter, P.; LaBonte, D.; Lamb, D. C.; Lan, N.; Liang, H.; Liao, H.; Liu, L.; Luo, C.; Lussier, M.; Mao, R.; Menard, P.; Ooi, S. L.; Revuelta, J. L.; Roberts, C. J.; Rose, M.; Ross-Macdonald, P.; Scherens, B.; Schimmack, G.; Shafer, B.; Shoemaker, D. D.; Sookhai-Mahadeo, S.; Storms, R. K.; Strathern, J. N.; Valle, G.; Voet, M.; Volckaert, G.; Wang, C. Y.; Ward, T. R.; Wilhelmy, J.; Winzeler, E. A.; Yang, Y.; Yen, G.; Youngman, E.; Yu, K.; Bussey, H.; Boeke, J. D.; Snyder, M.; Philippsen, P.; Davis, R. W.; Johnston, M., Functional profiling of the *Saccharomyces cerevisiae* genome. *Nature* **2002**, *418* (6896), 387-91.
32. Bens, M.; Vallet, V.; Cluzeaud, F.; Pascual-Letallec, L.; Kahn, A.; Rafestin-Oblin, M. E.; Rossier, B. C.; Vandewalle, A., Corticosteroid-dependent sodium transport in a novel immortalized mouse collecting duct principal cell line. *J Am Soc Nephrol* **1999**, *10* (5), 923-34.
33. Peters, K. W.; Qi, J.; Johnson, J. P.; Watkins, S. C.; Frizzell, R. A., Role of snare proteins in CFTR and ENaC trafficking. *Pflugers Arch* **2001**, *443 Suppl 1*, S65-9.
34. Qi, J.; Peters, K. W.; Liu, C.; Wang, J. M.; Edinger, R. S.; Johnson, J. P.; Watkins, S. C.; Frizzell, R. A., Regulation of the amiloride-sensitive epithelial sodium channel by syntaxin 1A. *J Biol Chem* **1999**, *274* (43), 30345-8.

35. Saxena, S. K.; George, C. M.; Pinskiy, V.; McConnell, B., Epithelial sodium channel is regulated by SNAP-23/syntaxin 1A interplay. *Biochem Biophys Res Commun* **2006**, *343* (4), 1279-85.
36. Collaco, A.; Marathe, J.; Kohnke, H.; Kravstov, D.; Ameen, N., Syntaxin 3 is necessary for cAMP- and cGMP-regulated exocytosis of CFTR: implications for enterotoxigenic diarrhea. *Am J Physiol Cell Physiol* **2010**, *299* (6), C1450-60.
37. Farinha, C. M.; Canato, S., From the endoplasmic reticulum to the plasma membrane: mechanisms of CFTR folding and trafficking. *Cell Mol Life Sci* **2017**, *74* (1), 39-55.
38. Schroder, M.; Kaufman, R. J., ER stress and the unfolded protein response. *Mutat Res* **2005**, *569* (1-2), 29-63.
39. Slominska-Wojewodzka, M.; Sandvig, K., The Role of Lectin-Carbohydrate Interactions in the Regulation of ER-Associated Protein Degradation. *Molecules* **2015**, *20* (6), 9816-46.
40. Alzayady, K. J.; Panning, M. M.; Kelley, G. G.; Wojcikiewicz, R. J., Involvement of the p97-Ufd1-Npl4 complex in the regulated endoplasmic reticulum-associated degradation of inositol 1,4,5-trisphosphate receptors. *J Biol Chem* **2005**, *280* (41), 34530-7.
41. Ye, Y.; Meyer, H. H.; Rapoport, T. A., Function of the p97-Ufd1-Npl4 complex in retrotranslocation from the ER to the cytosol: dual recognition of nonubiquitinated polypeptide segments and polyubiquitin chains. *J Cell Biol* **2003**, *162* (1), 71-84.
42. Alvarez de la Rosa, D.; Li, H.; Canessa, C. M., Effects of aldosterone on biosynthesis, traffic, and functional expression of epithelial sodium channels in A6 cells. *J Gen Physiol* **2002**, *119* (5), 427-42.
43. Wong, M. L.; Medrano, J. F., Real-time PCR for mRNA quantitation. *Biotechniques* **2005**, *39* (1), 75-85.